IEEE Access
Multidisciplinary | Rapid Review | Open Access Journal

Received September 6, 2017, accepted September 25, 2017, date of publication October 2, 2017,
date of current version November 7, 2017.

Digital Object Identifier 10.1109/ACCESS.2017.2758845

Model Structure Choice for a Static VAR Compensator Under Modeling Uncertainty and Incomplete Information

TETIANA BOGODOROVA[1], (Student Member, IEEE), AND LUIGI VANFRETTI[2], (Senior Member, IEEE)

[1]KTH Royal Institute of Technology, Stockholm 114 28, Sweden
[2]Electrical, Computer and Systems Engineering Department, Rensselaer Polytechnic Institute, Troy, NY 12180 USA

Corresponding author: Tetiana Bogodorova (tetianab@kth.se)

ABSTRACT To simulate the complex behavior of power systems, operators frequently rely on models. The task of model identification and validation becomes important in this context. The validity of the models has a direct influence on operator's decisions and actions. In other words, erroneous or imprecise models lead to erroneous predictions of the systems' behavior which may result in unwanted operator's actions. This paper addresses the challenge of model structure choice for modeling and parameter identification in power systems. Three types of model structures are analyzed: 1) physical principle-based modeling; 2) black-box modeling (NARX, transfer function, Hammerstein–Wiener model); and 3) combination of physical and black-box modeling. This analysis has been performed using real grid measurements and available knowledge about a static VAR compensator (SVC) connected to the U.K.'s transmission network and operated by National Grid. The SVC's modeling is presented in the context of a generalized modeling and identification algorithm, that is offered as a guideline for engineers. The model validity issues of the identified SVC models that include modeling uncertainty are discussed.

INDEX TERMS Black-box model, identification, model structure selection, parameter estimation, power system modeling, static VAR compensator.

I. INTRODUCTION

A. MOTIVATION

Mathematical modeling and parameter estimation of electric power grid components are important for power system operators [1]. An operator's ability to predict large blackouts [2] becomes a challenge when the models of real power system components contain uncertainties or deviations from their actual (real) observed behavior. This challenge is due in part by the complexity power system components, such as those of controllers and power electronic devices (e.g. Static VAR Compensator (SVC)). An SVC [3], [4], which is comprised by a controlled combination of discretely and continuously switched VAR sources, introduces complex non-linear dynamics. A SVC's dynamic transient response may contain unknown nonlinearities that are created by automated switching. In addition, the structural ambiguity of SVC appears due to the manufacturers secret ''know-how''.

Any lack of knowledge about the system has to be compensated by using mathematical data-based modeling, following the system identification cycle that is shown in Fig. 1. The system identification cycle deals with a problem of building a mathematical model based on the available information about the system.

The two main parts of the cycle are defined by: (1) decisions made by computer, and (2) decisions made by the engineer (Fig. 1), where the most challenging step is the model structure choice. The chosen model's structure will predefine what properties of the model can be identified (from measurements) and what behavior can be reproduced (by simulation).

Methods of model structure selection and parameter identification can be generally classified into two groups:

1) Physical principle-based modeling [3], and
2) Black-box mathematical modeling [6]–[8].

The physical principle-based modeling approach is well established in power system modeling. It is generally considered as more reliable due to its ability to reproduce the physical behavior of the system. However, with the advent of digital systems in control of physical processes, the power system components are governed by a combination of physical laws and control flows. Such components introduce

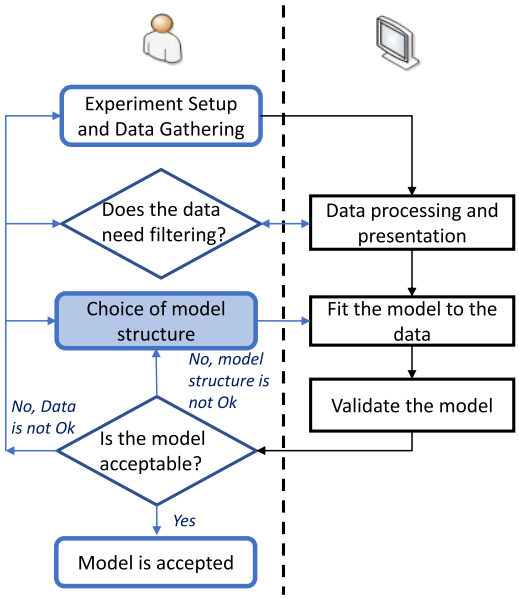

FIGURE 1. System identification cycle: computer's tasks (black) and engineer's tasks (blue) [5].

additional complex nonlinearities to the overall system. Thus, an engineer has to create a model that is sufficiently rich to reproduce such complex behavior. The families of flexible mathematical models that have no physical interpretation, but aim to describe input-output relationships of the system, are known as black-box models [6].

B. LITERATURE REVIEW

Among the many identification studies in power systems, the most relevant ones, that have been performed for SVC modeling, are summarized next. Authors in [9] present examples of transfer function identification including an SVC using the Prony TFI method. However, in comparison to our work, model order selection is not considered, meaning that the model structure is predefined in [9]. In contrast, our work addresses model order selection explicitly.

Seminal works have been pursued for SVC optimal control design using fuzzy logic-based algorithms [10], [11], and the tuning of its control parameters, considering predefined model structures [12], [13]. The nonlinear approximator used in these works is based on number of heuristic rules. The fuzzy logic-based modeling and identification requires tuning of fuzzy rule structure, and more attention to the ''curse of dimensionality'' problem is necessary that may be challenging for practicing engineers [14]. The methods that are presented in the proposed work do not experience such difficulties, as they do not depend on heuristics.

Advanced first principle-based models were developed using measurements and physical SVC characteristics in [3], [15]–[19]. The latter is possible only when complete or nearly-complete knowledge about the system (including an access to experiment design and exhaustive measurement gathering) is possible. In contrast, our work aims to address a more common circumstance, that is under incomplete information (i.e. limited model information and limited measurements). The nonlinear behavior of the SVC has been captured in [20] using advanced control designs to damp oscillations, but assuming a fixed standard model of the SVC is fully known. Differently, this work aims to study the identification of an SVC model that is largely unknown (i.e. for which there is only limited modeling information and measurements, that is, under incomplete information).

Harmonics present in sinusoidal signals has been evaluated using Fast Fourier-based algorithms [21] for reactive power compensation. In contrast, this article present different approaches for detailed model phasor-model identification using RMS voltage and current signals. In such type of models, harmonics are not of interest, but the dynamics are.

The problem of model structure choice for identification has been investigated extensively in the control and system identification communities [5], [7]. However, in respect to all the reviewed works [10]– [21], these practices have not yet been studied, applied and adopted in the power systems community.

C. CONTRIBUTION

This paper compares and discusses model structure choice methods in the context of a modeling and parameter identification cycle that can be applied for the modeling of power system components. These methods are physical principle-based modeling; and black-box mathematical modeling (Nonlinear AutoRegressive Exogenous (NARX) [22], Transfer function [23], Hammerstein-Wiener model [5]). In addition, the combination of physical principle-based and black-box modeling is proposed. All the case studies have been performed by modeling a Static VAR Compensator, for which real measurements from the grid were available, while the information about the physical system and control flow that governs its behavior was limited (or incomplete).

Furthermore, this article discusses how modeling uncertainty can be considered by an engineer: by evaluating the validity of a model, it is possible to justify the model's acceptance. Using Static VAR Compensator model case study, the paper reveals a number of important issues that should be addressed during the identification process, and proposes possible solutions.

D. PAPER ORGANIZATION

The remainder of this article is structured as follows. Section II offers a modeling problem formulation using the SVC's measurement data. Section III compares model structure choice methods. Section IV describes the identification methodology and validity criteria used for the proposed models. Section V presents the modeling methodology which is applied for the SVC's modeling problem. Section VI discusses model acceptability issues. Section VII sums up results and draws conclusions.

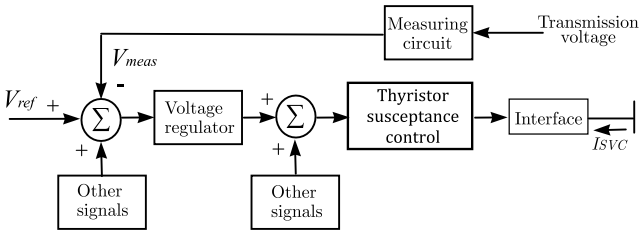

FIGURE 2. Physical principle-based SVC model.

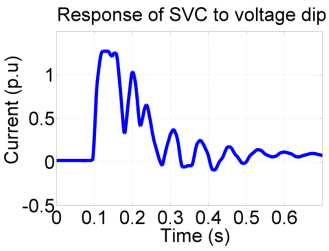

FIGURE 3. SVC RMS current.

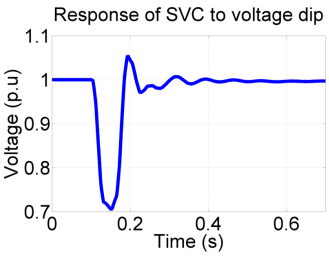

FIGURE 4. SVC RMS voltage.

II. STATIC VAR COMPENSATOR MODELING PROBLEM FORMULATION

The system identification problem can be formulated as: *identify the system's model in a way that it reproduces the system behavior known from a description of the system and collected measurement data.*

The Static VAR Compensator system (Fig. 2) is a combination of a shunt capacitor bank and a thyristor-controlled shunt reactance aimed to inject reactive power for controlling the voltage at the directly connected bus-bars or remote bus-bars. For the SVC example used here, the system description provided by National Grid, was limited to name-plate data for the thyristor-controlled reactor (TCR) (reactive power generated), thyristor-switched capacitors (TSC) and mechanically-switched capacitor (MSC). In addition, the SVC is voltage controller with a droop of 4% under balanced operation conditions is applied. Because the provided measurements that were received correspond to a transient response, and they do not include reactive power measurements on the controlled bus bar, the voltage set point is assumed to be fixed.

The provided measurements include the SVC's current (Fig. 3) and voltage (Fig. 4), recorded after a single phase (IB) fault occurred. During the voltage dip the thyristor-switched capacitors are activated to limit the voltage drop.

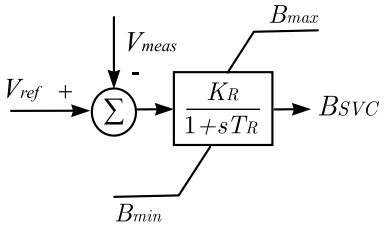

FIGURE 5. IEEE SVC Type 1 [4].

The dynamics of the SVC become active and they can be identified from the provided measurements. The sampling time of the recordings is 0.0001 s (i.e. 10 kHz).

III. MODEL STRUCTURES

In the identification cycle (see Fig. 1), the choice of possible model structures is no doubt the most important and the most difficult step for an engineer. In this section, different modeling approaches are discussed.

A. PHYSICAL PRINCIPLE-BASED MODELING

The most common modeling method is grounded on the established laws of physics that are considered axiomatic. On this level of modeling, no empirical model assumptions or fitting parameters are made [24].

For the particular SVC the limited information, available to National Grid (who operates the SVC), leads to the use of the basic IEEE SVC regulator model [4] (see Fig. 5).

In power systems the main issue the engineer faces with such type of modeling is partially available (limited) or unavailable information about the structure of the component and the system as a whole. There are several reasons for that: a) component producers protect their "know-how", b) the system is old and installations/changes to the components are poorly documented, c) control systems at different levels of control hierarchy become digital with complex logical actions, some dependent on operator's decisions; to list a few.

This model structure choice has been guided by the available information about the SVC system. In this case, only a droop that defines the voltage dependency on reactive power set point was known. However, the known physical characteristics of SVC [3] can help to define the range of the time constants. To sum up, the set of parameters to be identified in this case is $\theta = [K_R, T_R]$.

B. BLACK-BOX MODELING

Observing the SVC's response, it can be concluded that the transient characteristics of the SVC RMS current and voltage (Fig.3, 4) show a non-linear behavior combined with the linear component of a set of differential equations (involving the under-damped transient oscillatory behavior of at least two complex modes). This gives ground to apply mathematical (black-box) modeling methods for the SVC's model identification.

FIGURE 6. Hammerstein-Wiener (HW) model.

1) HIGH ORDER TRANSFER FUNCTION MODEL

Usually SVC dynamics involve different time-scales and include their voltage regulator [25], consequently, a high order transfer function model is appropriate in this case. If the relation between input and undisturbed output can be written as a linear difference equation, and the disturbance consists of white measurement noise [5], then the ARX model can be expressed using an Output-Error (OE) model structure of the form:

$$\begin{aligned} y(t) &= \frac{B(q)}{F(q)}u(t-n_k) + e(t) \\ F(q) &= 1 + f_1 q^{-1} + \ldots + f_{n_f} q^{-n_f} \\ B(q) &= b_1 q^{-1} + \ldots + b_{n_b} q^{-n_b} \end{aligned} \tag{1}$$

The unknown values are the transfer function parameters $\theta = [b_1\ b_2 \ldots b_{n_b}\, f_1\, f_2 \ldots f_{n_f}]$ and transfer functions of order n_b, n_f, n_k.

2) HAMMERSTEIN-WIENER MODEL

In order to include the nonlinear dynamic behavior that is observed in the measurements, the Hammerstein-Wiener model is exploited (Fig.6).

The OE model structure (1) is included in the linear block, while the input nonlinearity by a piecewise linear function:

$$w = \Phi(u, \theta_{pwl}) = (u - u_i)\frac{(w_{i+1} - w_i)}{(u_{i+1} - u_i)} + w_i \tag{2}$$

where $\{w_i \le |w| \le w_{i+1};\ u_i \le |u| \le u_{i+1}\}_{i=1..k}$ are the limits of the input x and output nonlinearity y values for each interval; k - number of beakpoints; $\theta_{pwl} = [\{u_1, w_1\}, \ldots \{u_k, w_k\}]$ - identified parameters.

From the physical principle-based modeling in Fig. 5 susceptance variation limits introduce to model the SVC's saturations. These limits are modeled using the saturation function (3) that has been introduced as output nonlinearity in the Hammerstein-Wiener model.

$$y = S(x, B_{max}, B_{min}) = \begin{cases} x(t), & \text{if } B_{min} < x(t) < B_{max} \\ B_{max}, & \text{if } x(t) \ge B_{max} \\ B_{min}, & \text{if } x(t) \le B_{min} \end{cases} \tag{3}$$

Observing the current measurement (Fig. 3), the upper bound given by the B_{max} value is reached during the event.

3) NONLINEAR AUTOREGRESSIVE eXogenous (NARX) MODEL

This model represents the system's linear and nonlinear behavior as a sum of an ordinary ARX and the complex wavelet function over a set of chosen regressors. The nonlinear ARX model (Fig.7) includes two parts:

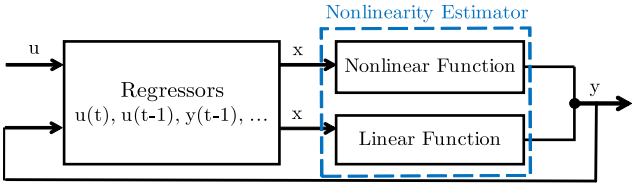

FIGURE 7. Nonlinear AutoRegressive eXogenous model.

- Regressors from the current $u(t)$ and past input values $u(t-1), u(t-2), \ldots, u(t-m_u)$ and past output data $y(t-1), y(t-2), y(t-3), \ldots, y(t-m_y)$; while letting $x = [y(t-1), y(t-2), y(t-3), \ldots, y(t-m_y), u(t), u(t-1), u(t-2), \ldots, u(t-m_u)]$ be a $1 \times m$ vector of regressors.
- A nonlinearity estimator that maps regressors to the model output, shown in Fig. 7.

The nonlinear ARX model estimator is given by:

$$\hat{y}(t|\theta) = [-a_1, -a_2, \ldots, -a_{n_a}, b_1, b_2, \ldots, b_{n_b}] * x^T + d + \Gamma(x, \theta_{NL}), \tag{4}$$

where $\theta_L = [a_1 a_2 \ldots a_{n_a} b_1 b_2 \ldots b_{n_b}]^T$ - parameters of ARX linearity estimator, n_a - number of past output terms, n_b - number of past input terms, d - a scalar offset.

In this case, the nonlinear behavior is represented by the wavenet function $\Gamma(x, \theta_{NL})$ [26]:

$$\begin{aligned} \Gamma(x, \theta_{NL}) = {} & a_{s_1} f(b_{s_1}((x-r)Q - c_{s_1})) \\ & + \ldots + a_{s_{ns}} f(b_{s_{ns}}((x-r)Q - c_{s_{ns}})) \\ & + a_{w_1} g(b_{w_1}((x-r)Q - c_{w_1})) \\ & + \ldots + a_{w_{nw}} g(b_{w_{nw}}((x-r)Q - c_{w_{nw}})) \end{aligned} \tag{5}$$

where $f(z) = e^{-0.5zz^T}$ is a scaling function, $g(z) = (m - zz^T)e^{-0.5zz^T}$ is a wavelet function, z - $1 \times q$ vector with q - number of x components used in the scaling and wavelet functions; Q - $m \times q$ projection matrix; r - $(1 \times m)$ mean values of regressor vector; a_s $(n_s \times 1)$, b_s $(n_s \times 1)$, c_s $(n_s \times q$ vector) - scaling parameters; a_w $(n_w \times 1)$, b_w $(n_w \times 1)$, c_w $(n_w \times q)$ - wavelet parameters. $\theta_{NL} = [Q, r, a_s, b_s, c_s, a_w, b_w, c_w]$ - parameters of nonlinearity estimator. The number of units is equal to the sum of scaling (n_s) and wavelet (n_w) coefficients.

When estimating a nonlinear ARX model, the model parameter values $\theta = [\theta_L, \theta_{NL}, d]$ are computed.

IV. PARAMETER IDENTIFICATION AND MODEL VALIDATION CRITERIA

The optimization criterion to be met in the all the model structure choices is the minimisation of the mean squared error (MSE) between measured and simulated outputs:

$$\hat{\theta}_N = \underset{\theta}{\operatorname{argmin}} \frac{1}{N}\sum_{i=1}^{N}(y_i(t) - \hat{y}_i(t|\theta))^2 \tag{6}$$

where $y_i(t)$ - measured response, $\hat{y}_i(t|\theta)$ - estimated response, N - number of samples. In the sequel, the output y_i or $\hat{y}_i$ dependency on time t and parameters θ will be omitted.

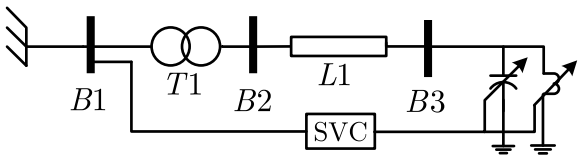

FIGURE 8. SVC connected to grid model.

The goodness of fit criterion to evaluate how well the estimated model response fits to the measured output is quantified in percentage of the two curves' alignment as Normalized Mean Squared Error (NMSE) (7):

$$Fit = NMSE(\theta, y) = \left(1 - \frac{\sqrt{\frac{1}{N}\sum_{i=1}^{N}(y_i - \hat{y}_i)^2}}{\sqrt{\frac{1}{N}\sum_{i=1}^{N}(y_i - \bar{y}_i)^2}}\right)100\% \quad (7)$$

where $\bar{y}_i$ - mean value of the response.

The Akaike information criterion (AIC), applied to model order selection, includes the minimization of MSE and a model complexity penalty [27], [28]. One of its versions can be formulated in the following way:

$$AIC(\rho) = Nln(MSE(\theta)) + \rho n \quad (8)$$

where n - number of system parameters (characterizing the order of the system) and ρ - regularization coefficient, which is usually equal to 2.

The algorithm for parameter identification [29] is used herein to meet the optimization criterion by iteratively adjusting model parameters when the chosen model structure and optimization algorithms (search methods)[1] are given.

V. RESULTS

In this section the results of applying the model identification methodology discussed above is presented. There are several modeling scenarios discussed:

A First principle modeling (Section V-A)
B Black-box modeling (Sections V-B, V-C, V-D)
C Combination of both A and B models (Section V-E)

A. PHYSICAL FIRST PRINCIPLE-BASED MODELING

To reproduce the actual (real) power system behavior using the physical principle modeling approach, a power system model developed using Modelica was built [30]. The model contains an SVC Type 1 connected via a transmission line and transformer to a 400 kV substation (Fig. 8). A single phase fault is applied to the transformer from the SVC side on bus B2. The equivalent of the external grid has been modeled as an infinite bus.

The parameters (K_R, T_R) range is [20..100] (corresponding to a droop from 5% to 1%) and [20..150] *ms* [31]. Assuming that B_{SVC} is proportional to the current injection with a voltage of 1 *p.u.* measured at the bus bar B1, the parameter estimation results are summarized in Table 1.

[1]The choice of the search methods is out of scope of this paper. However, for more information, refer to [5], [14].

TABLE 1. Estimated parameters for the IEEE SVC Type 1.

	$[T_R]^{(0)}$	$[K_R]^{(0)}$	K_R	T_R	MSE
1	0.02	[20..50]	0.02	[22.19..27.27]	0.0274
2	0.02	[50..70]	0.02	[50.37..51.75]	0.0286
3	0.02	[70..100]	0.02	[70.14..70.68]	0.0297
4	0.15	[20..50]	0.15	49.51	0.0276
5	0.15	[50..70]	0.15	[69.46..69.94]	0.0231
6	0.15	[70..100]	0.15	[97.50..99.65]	0.020
7	[0.02..0.15]	[20..100]	0.104 0.108 0.123	99.88 [98.02..98.86] [97.40..97.52]	0.0193

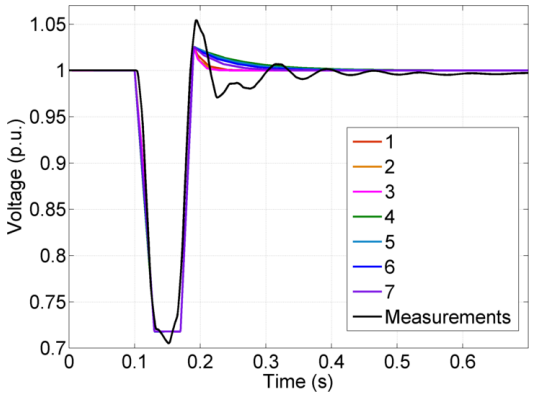

FIGURE 9. Simulated physical principle-based model output against the measured SVC RMS voltage. The legend corresponds to the cases in Table 1.

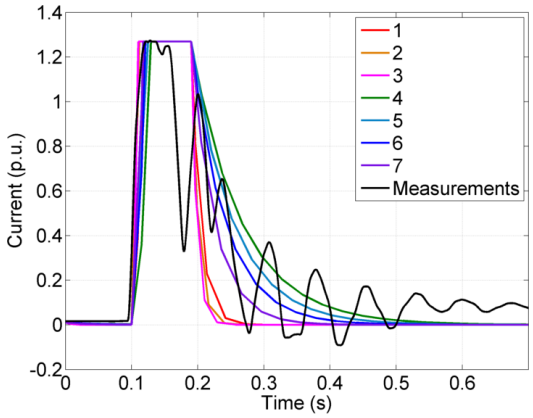

FIGURE 10. Simulated physical principle-based model output against the measured SVC RMS current. The legend corresponds to the cases presented in Table 1.

As shown in Table 1, seven different initial parameter conditions have been set to identify the parameter values (K_R, T_R) that correspond to the minimal MSE in the chosen initial parameter range ($[K_R]^{(0)}$, $[T_R]^{(0)}$). The MSE values have been evaluated using both the SVC's voltage and current outputs (Figs. 9, 10).

Considering estimated outputs of the SVC voltage and current (Figs. 9, 10) together with the results in Table 1, several observations can be made. As expected, the rise in the slope of the current is influenced mainly by the gain K_R

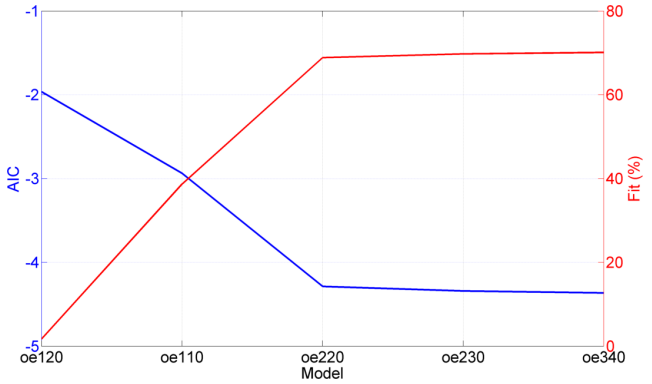

FIGURE 11. Model $OE(n_b, n_f, n_k)$ order choice using AIC and NMSE criteria.

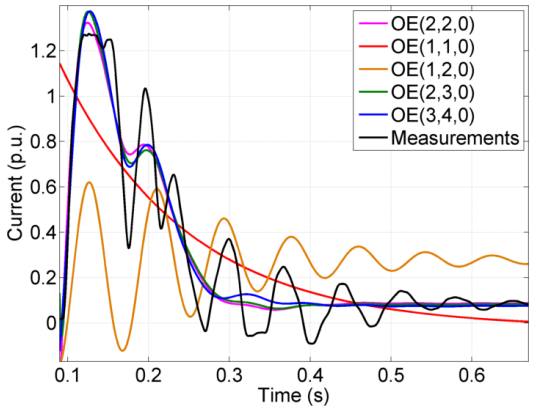

FIGURE 12. Simulated $OE(n_b, n_f, n_k)$ model output against measured SVC RMS current.

value. The higher the gain, the faster the rise (or a steeper slope). On the contrary, the falling slope depends on the time constant T_R that defines the speed of exponential decay before reaching a steady-state condition. The first order transfer function can't reproduce the oscillatory behavior shown by the measurements. Nevertheless, the average descent curve is obtained. Summing up, the slower descent and higher gain from the initial values in Case 7 (Table 1) gives the best estimates in terms of minimizing the MSE (6). This model is summarized in Table 2.

B. HIGH ORDER TRANSFER FUNCTION

To achieve a better model output, a higher order transfer function is used next as a model structure. The model is linear, but saturation can be added in series as separate function to model the nonlinearity. In the case of OE model structure (1), the most important decision for an engineer is the choice of model's order. The aim is to obtain the best fit possible while keeping the model order as low as possible. For this purpose, an experiment on the model order selection has been carried out by employing two criteria of goodness of fit: the Akaike information criterion (AIC) (8), and the NMSE (7) (or Fit (%) on the plots).

In Fig. 11 the rapid fall of the AIC value indicates an improvement on the model's fitness. This occurs starting with the model order of $n_b = 2, n_f = 2, n_k = 0$ (x-axis). Therefore, three models (`oe220`: $OE(2, 2, 0)$, `oe230`: $OE(2, 3, 0)$, `oe340`: $OE(3, 4, 0)$) show a good fit. $OE(2, 3, 0)$ model is added to Table 2. Considering the fitting results of the SVC's current in Fig. 12, all of the three aforementioned models give a better representation of the dynamics when comparing with the SVC Type 1 model (Fig. 10), but it requires improvements to capture the nonlinear behavior of the system (see Sections V-C, V-D).

C. HAMMERSTEIN-WIENER (HW) MODEL

The Hammerstein-Wiener model (Fig. 6) includes input and output nonlinearities together with a linear component. In Section V-B, one of the models that show the best fit was of $n_b = 2, n_f = 3, n_k = 0$ order. Therefore, it was selected as a

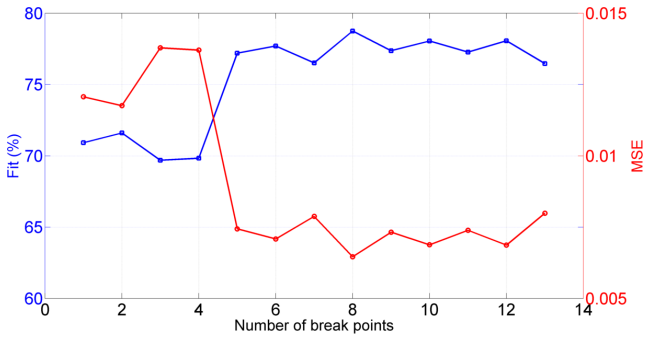

FIGURE 13. HW model: NMSE (Fit,%) and MSE dependency on the number of breakpoints.

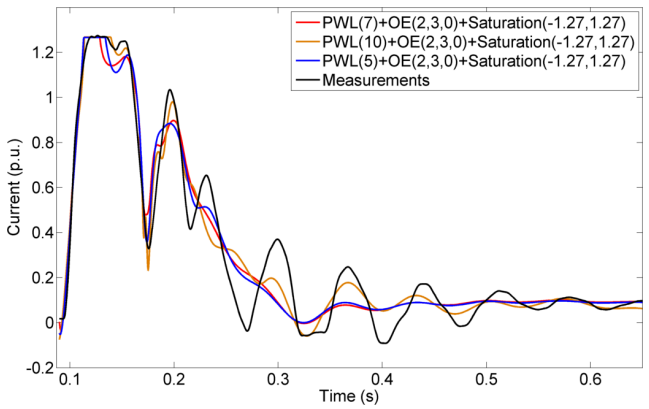

FIGURE 14. HW model with piecewise linear input and saturation function output compared to the measured SVC RMS current.

linear component. The output nonlinearity has been modeled using a saturation function with upper/lower limits equal to ± 1.27 $p.u.$. The remaining (unexplained) dynamics are modeled using an input piecewise linear function. However, the latter has to be defined by the number of break points k and their location $(x_i, y_i)_{i=1..k}$ (2). Input x_i values are SVC voltage measurements, while y_i are the nonlinearity values.

To choose the appropriate number of break points of the piecewise linear function (2), a study on dependency of the

TABLE 2. Numerical experiment results.

Section	Model Structure	Est. Parameters	MSE	NMSE (Fit,%)
V. A	SVC Type I	$K_R = 0.104,\ T_R = 99.88$	0.0193	55.52
V. B	TF	$n_b = 2; n_f = 3; n_k = 0$	0.0130	69.77
V. C	HW	$n_b = 2; n_f = 3; n_k = 0;\ k = 10;$ $saturation = \pm 1.27$	0.0069	78.05
V. D	NARX	$n_s + n_\omega = 17;\ n_b = 2; n_f = 2; n_k = 1$	0.0061	79.24
V. E	SVC Type I + NARX	V. A + V. D Est. parameters	0.0059	84.27

Acronyms: TF - transfer function, Est. - estimation, HW - Hammerstein-Wiener

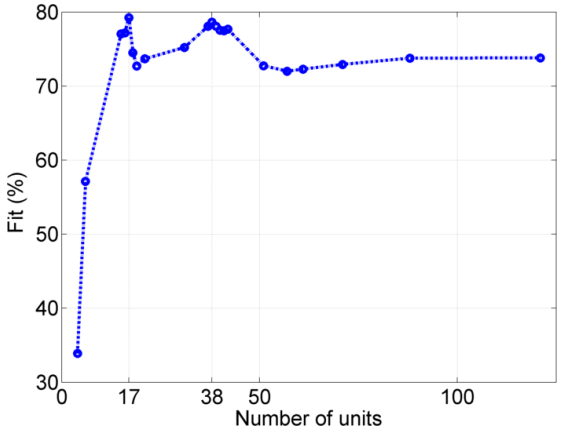

FIGURE 15. NARX: Fit,% dependency on number of wavenet units.

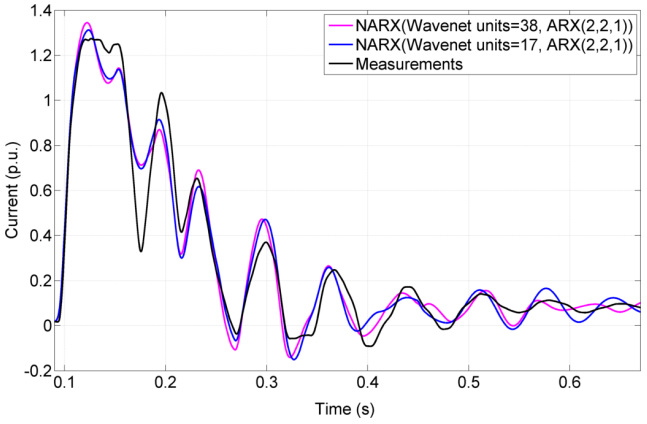

FIGURE 16. NARX models output from 17 and 38 wavenet units compared to the measured SVC RMS current.

goodness of fit metric (and MSE) on the number of break points has been performed (see Fig. 13). The principle used to make a choice is to obtain a simple model (aiming for the minimum number of break points) capable of providing a high goodness of fit (and small MSE). In Fig. 13 the steep rise of the fit (in percentage) occurs when 5 break points of the piecewise linear function are included. After 5 break points, the fit value does not change drastically. Therefore, the 5 break points piecewise linear function can be considered as an adequate number of points to model the nonlinearity. To increase certainty in the choice of the model, three models with $k = 5$, $k = 7$ and $k = 10$ break points of the piecewise linear function have been compared (Tables 3, 4, 5 and Fig. 14). As expected, the model with $k = 10$ break points (see Table 2) has reproduced the dynamics better than those of $k = 5$ and $k = 7$.

D. NONLINEAR AUTOREGRESSIVE eXogenous (NARX) MODEL

The NARX model is designed by applying a wavelet network (wavenet) function to an input vector of regressors. Two input parameters are required to define the model structure before the estimator identifies other parameters automatically. The order of the linear function (discussed in Section V-B) and the number of wavenet units $(n_s + n_\omega)$ (5). The latter has been evaluated in terms of the maximization of the goodness of fit (*Fit* (%)) and shown in Fig. 15. In Fig. 15 two values in the range of the analyzed wavenet units values are of interest. Both models with $(n_s + n_\omega = 17)$ and $(n_s + n_\omega = 38)$ wavenets units with the highest fit have been compared on their ability to capture the dynamics of measurements in the SVC current output (Fig. 16). The model comprised by 17 units is capable to represent the oscillation frequencies more precisely than the 38 units model. The simplest (lower order model) is always preferred. In this case the $(n_s+n_\omega = 17)$ units model is the best choice (see Table 2). The linear ARX part has been chosen with the criteria of having the lowest order that provides a high fitness.

E. COMBINATION OF MODELS

The physical principle-based model (Section V-A) is able to reproduce the main physical properties of SVC system, even though it doesn't include all the observed dynamics for the particular measured event. In contrast, the black-box mathematical model is capable to reproduce the system dynamics of the event with good fitness (Fig. 14, 16). The ability to combine both models is advantageous in the sense of preserving both an insight about the system physical properties together with the best goodness of fit.

To this aim this section proposes to design a switch that will allow to substitute the physical model with one of the other models in Table 2, when needed. The steady-state operation can be represented by the well established IEEE SVC Type 1 model, while transient dynamics excited in the event have to be modeled by the richer mathematical

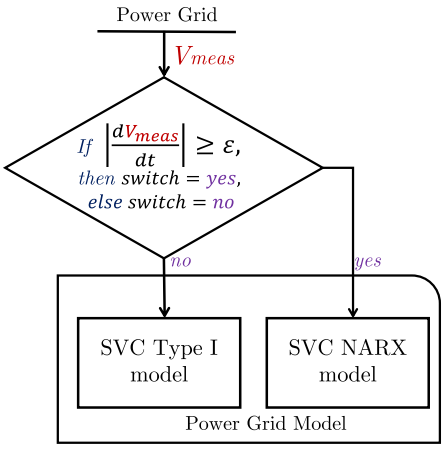

FIGURE 17. Switch operational principle combining two model types.

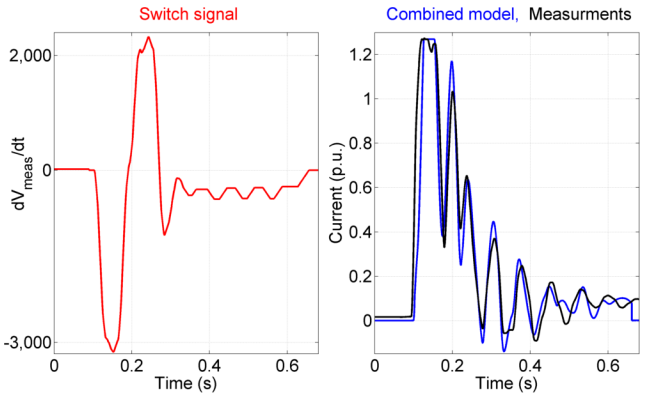

FIGURE 18. Combined model: switch operation and model response.

models presented in the previous sections (e.g. HW model or NARX).

The operational principle of the switch (Fig. 17) takes a derivative of the voltage input signal and decides to switch between the IEEE SVC Type 1 model and a mathematical model when the voltage derivative crosses a given threshold defined by an engineer.

To realize the switch the following aspects need to be considered. First, the input is a nonlinear function that is not differentiable across the entire time span. The solution to this issue is to compute numerically the derivative with the substitution of infinity by a large number to limit the derivative values to certain real-valued bounds. The operation of the switch does not require precise derivative values (unless it influences the switch's operation). The threshold value (ϵ) is chosen equal to 0.05 and modeled using a dead zone function.

Second, it is necessary to avoid the switching before the steady-state is reached. When small deviations or oscillations around the steady-state point are still present in the system (Fig. 4), the voltage derivative oscillates around zero. This is solved by implementing a direct discrete FIR filter of order equal to the signal's sampling frequency multiplied by the time window over which the steady-state is reached. In other words, the filter finds the cumulative sum of the derivative value over the time window.

Finally, the output filtered dead zoned derivative signal, when not equal to zero, activates the switch from the IEEE SVC Type I model to the SVC NARX model (Fig. 18). In Fig. 18 the combined model's output compared to measurements is presented. The observed fitness (Fig. 18) and evaluated model validation criteria (Table 2) show better performance than all other studied models (see Sections V.A-V.D).

VI. DISCUSSION

The most difficult decision that an engineer is responsible for is model acceptance (Fig. 1). When this can not be achieved, an engineer should list all the concerns on the model's quality in terms of validation metrics and case studies. If the model

TABLE 3. Break points (BP) values of $k = 5$ (2) (Fig. 6).

	BP 1	BP 2	BP 3	BP 4	BP 5
x_i	0.7909	0.8740	0.8893	0.9498	1.0066
y_i	−0.0001	0.0004	0.0005	0.0001	0.0001

TABLE 4. Break points (BP) values of $k = 7$ (2) (Fig. 6).

	BP 1	BP 2	BP 3	BP 4	BP 5	BP 6	BP 7
x_i	0.6308	0.7912	0.8112	0.8826	0.9282	0.9517	1.0052
y_i	0.0005	−0.0001	0.0002	0.0002	0.0006	0.0002	0.0002

is accepted, the conditions when the model is valid should also be defined. All the limitations and advantages of the model have to be carefully listed. The quantitative methods and metrics used in this work can be used for these purposes.

Incomplete modeling information and/or measurement limits the system properties that are reproduced by a model. To obtain a precise model (in this case for the SVC), a highly dynamic input excitation signal $u(k)$ (V_{ref} or V_{meas} Fig. 2) needs to be available. Alternatively, proper excitation signal design [32], [33] allows to gather as much information about the system as possible. In the particular case studies (Sections II, V), all the chosen model structures have been chosen for the only available measurements (Fig. 3, 4) and the limited information available to the grid operator itself (National Grid). The assumption is that the all possible dynamics have been excited. No doubt that when the experiment design is controlled by an engineer, better certainty for the estimated model can be given.

One more issue that has to be taken into consideration is the change of the operation point after an event (Fig. 10). It can be estimated by computing power flow values or by back calculating them from the available measurements [5]. In this paper, it was assumed (from information available from National Grid) that the steady-state operation conditions did not change after the event.

The proposed combined model allows to use mathematical black-box model (i.e. NARX in this study) when the first principle-based model fails to capture the dynamics present in

TABLE 5. Break points (BP) values of $k = 10$ (2) (Fig. 6).

	BP 1	BP 2	BP 3	BP 4	BP 5
x_i	0.7373	0.7664	0.8001	0.8321	0.8648
y_i	−0.0000	0.0002	−0.0007	0.0022	−0.0030
	BP 6	BP 7	BP 8	BP 9	BP 10
x_i	0.8953	0.9301	0.9703	0.9926	1.0279
y_i	−0.0024	0.0000	0.0001	0.0002	0.0001

the grid. These dynamics are excited by the events that force the system deviate from near steady-state operation. Considering the fitness criteria defined in this paper, the method is superior to all other methods that are compared in Table 2.

VII. CONCLUSION

In this paper, methods for model structure choice in power system component model identification have been discussed. The traditional physical principle-based modeling approach gives a good representation only in the absence of uncertainty. Meanwhile, when the knowledge of the system or its component is limited, the physical principle modeling fails to reproduce the system dynamics in the model. Therefore, mathematical black-box and grey-box modeling techniques can be exploited. This work proposed to combine both model types, using the simplest one when the dynamics of the system are not excited, i.e. in steady-state operation. Meanwhile, more complex mathematical nonliner models can be used when nonlinearities arise. All the case studies (Table 2) have been illustrated using the RMS voltage and current recordings and incomplete modeling information of an SVC operated by National Grid.

APPENDIX

Output-Error (OE) model structure: The selected model $n_b = 2, n_f = 3, n_k = 0$. The assumption is that there is no delay ($n_k = 0$).

$$B(q) = 0.0003645 - 0.0003644q^{-1};$$
$$F(q) = 1 - 2.959q^{-1} + 2.917q^{-2} - 0.9587q^{-3}$$

NARX: Model parameter values $\theta = [\theta_L, \theta_{NL}, d]$: Standard regressors corresponding to the orders: $n_a = 2, n_b = 2$. $\theta_L = [a_1\ a_2\ b_1\ b_2] = [0.3770\ -0.0087\ 0.0028\ 0]$. Nonlinear regressors: $u(t-1), u(t-2)$ Nonlinearity estimator $\theta_{NL} = [Q, r, a_s, b_s, c_s, a_w, b_w, c_w]$: $Q = [0\ 0; 0\ 0; -6.5\ -2700.9; -6.5\ 2700.9]$; $r = [0.2813\ 0.2813\ 0.9709\ 0.9709]$; wavenet with 17 units: scaling $n_s = -2.7301 \times 10^{-4}$ and wavelet $n_w = 10^{-3} \times [0.3035\ -0.0489\ -0.0344\ -0.1723\ -0.0203\ -0.0271\ 0.0696\ 0.0588\ -0.0179\ 0.0150\ -0.0076\ 0.0080\ 0.0335\ 0.0121\ -0.0766\ 0.0210]$ coefficients.

A scalar offset $d = 0.2814$.

Hammerstein-Wiener models that defined by θ_{pwl} are presented for order $k = 5$ (Table 3), $k = 7$ (Table 4), $k = 10$ (Table 5):

ACKNOWLEDGMENT

The authors are thankful to Parry Batth and Andrew Kensley of National Grid who kindly provided the few available measurements and SVC's modeling structure information during the FP7 iTesla project [34], and the challenge to develop the solutions presented within this paper.

REFERENCES

[1] R. Memisevic, A. Kamberovic, and A. Kenwrick, "Validation and calibration of the blackwall SVC AVR and POD models," in *Proc. Austral. Univ. Power Eng. Conf.*, Sep. 2016, pp. 1–6.

[2] B. Agrawal and D. Kosterev, "Model validation studies for a disturbance event that occurred on June 14 2004 in the western interconnection," in *Proc. IEEE Power Eng. Soc. Gen. Meet.*, Jun. 2007, pp. 1–5.

[3] P. Pourbeik *et al.*, "Generic model structures for simulating static VAr systems in power system studies—A WECC task force effort," *IEEE Trans. Power Syst.*, vol. 27, no. 3, pp. 1618–1627, Aug. 2012.

[4] F. Milano, "Power system analysis toolbox manual-documentation for PSAT version 2.1.6," Univ. College Dublin, Dublin, Ireland, Tech. Rep., May 2010.

[5] L. Ljung, *System Identification: Theory for the User*. Englewood Cliffs, NJ, USA: Prentice-Hall, 2009.

[6] I. Kamwa, G. Trudel, and L. Gerin-Lajoie, "Low-order black-box models for control system design in large power systems," in *Proc. IEEE Power Ind. Comput. Appl. Conf.*, May 1995, pp. 190–198.

[7] L. Ljung, "Black-box models from input-output measurements," in *Proc. 18th IEEE Instrum. Meas. Technol. Conf.*, vol. 1. May 2001, pp. 138–146.

[8] R. K. Pearson and M. Pottmann, "Gray-box identification of block-oriented nonlinear models," *J. Process Control*, vol. 10, no. 4, pp. 301–315, 2000.

[9] J. R. Smith, F. Fatehi, C. S. Woods, J. F. Hauer, and D. J. Trudnowski, "Transfer function identification in power system applications," *IEEE Trans. Power Syst.*, vol. 8, no. 3, pp. 1282–1290, Aug. 1993.

[10] J. Lu, M. H. Nehrir, and D. A. Pierre, "A fuzzy logic-based adaptive damping controller for static VAr compensator," *Electr. Power Syst. Res.*, vol. 68, no. 2, pp. 113–118, 2004.

[11] T. Abdelazim and O. P. Malik, "Intelligent SVC control for transient stability enhancement," in *Proc. IEEE Power Eng. Soc. Gen. Meet.*, vol. 2. Jun. 2005, pp. 1701–1707.

[12] A. Safa and M. Sakhaeifar, "Mismatched disturbance attenuation control for static VAr compensator with uncertain parameters," *Int. J. Elect. Power Energy Syst.*, vol. 91, pp. 61–70, Oct. 2017.

[13] C. A. O. Medina and J. A. O. Vélez, "SVC-POD tuning methodology and application to a Colombian case," in *Proc. IEEE Texas Power Energy Conf. (TPEC)*, Feb. 2017, pp. 1–6.

[14] O. Nelles, *Nonlinear System Identification*. Berlin, Germany: Springer, 2010.

[15] G. Reed *et al.*, "Technical requirements and design of the indianapolis power & light 138 kV southwest static VAr compensator," in *Proc. IEEE/PES Transmiss. Distrib. Conf. Expo.*, May 2016, pp. 1–5.

[16] W. H. Wellssow, M. Ostermann, H. Acker, W. Heckmann, and D. Cremer, "Advanced model of static VAr compensators for power flow calculations," in *Proc. IEEE PES Innov. Smart Grid Technol. Conf. Eur.*, Oct. 2016, pp. 1–6.

[17] H. Jin, G. Goos, and L. Lopes, "An efficient switched-reactor-based static VAr compensator," *IEEE Trans. Ind. Appl.*, vol. 30, no. 4, pp. 998–1005, Jul. 1994.

[18] A. N. Vasconcelos, A. J. P. Ramos, J. S. Monteiro, M. V. B. C. Lima, H. D. Silva, and L. R. Lins, "Detailed modeling of an actual static VAr compensator for electromagnetic transient studies," *IEEE Trans. Power Syst.*, vol. 7, no. 1, pp. 11–19, Feb. 1992.

[19] F. M. Gonzalez-Longatt, "Evaluation of reactive power compensations for the phase I of Paraguana wind based on system voltages," in *Proc. 39th Conf. IEEE Ind. Electron. Soc.*, Nov. 2013, pp. 1627–1631.

[20] R. Fazal and M. Choudhry, "Design of non-linear static VAr compensator based on synergetic control theory," *Electr. Power Syst. Res.*, vol. 151, pp. 243–250, Oct. 2017.

[21] O. F. Kececioglu, A. Gani, and M. Sekkeli, "A performance comparison of static VAr compensator based on goertzel and FFT algorithm and experimental validation," *SpringerPlus*, vol. 5, no. 1, p. 391, 2016.

[22] S. A. Billings, *Nonlinear System Identification: NARMAX Methods in the Time, Frequency, and Spatio-Temporal Domains*. Hoboken, NJ, USA: Wiley, 2013.

[23] G. E. Box, G. M. Jenkins, G. C. Reinsel, and G. M. Ljung, *Time Series Analysis: Forecasting and Control*. Hoboken, NJ, USA: Wiley, 2015.

[24] L. Ljung and T. Glad, *Modeling of Dynamic Systems*. Englewood Cliffs, NJ, USA: Prentice-Hall, 1994.

[25] D. Lijie, L. Yang, and M. Yiqun, "Comparison of high capacity SVC and STATCOM in real power grid," in *Proc. Int. Conf. Intell. Comput. Technol. Autom.*, vol. 1. May 2010, pp. 993–997.

[26] Q. Zhang, "Using wavelet network in nonparametric estimation," *IEEE Trans. Neural Netw.*, vol. 8, no. 2, pp. 227–236, Mar. 1997.
[27] H. Akaike, "A new look at the statistical model identification," *IEEE Trans. Autom. Control*, vol. AC-19, no. 6, pp. 716–723, Dec. 1974.
[28] V. S. Peric, T. Bogodorova, A. N. Mete, and L. Vanfretti, "Model order selection for probing-based power system mode estimation," in *Proc. IEEE Power Energy Conf. Illinois (PECI)*, Feb. 2015, pp. 1–5.
[29] L. Vanfretti, T. Bogodorova, and M. Baudette, "Power system model identification exploiting the Modelica language and FMI technologies," in *Proc. IEEE Int. Conf. Intell. Energy Power Syst. (IEPS)*, Kyiv, Ukraine, Jun. 2014, pp. 127–132.
[30] L. Vanfretti, T. Rabuzin, M. Baudette, and M. Murad, "iTesla power systems library (iPSL): A Modelica library for phasor time-domain simulations," *SoftwareX*, vol. 5, pp. 84–88, Dec. 2016. [Online]. Available: https://github.com/ElsevierSoftwareX/SOFTX-D-16-00027
[31] C. Taylor, G. Scott, and A. Hammad, "Static VAr compensator models for power flow and dynamic performance simulation," *IEEE Trans. Power Syst.*, vol. 9, no. 1, pp. 229–240, Feb. 1994.
[32] V. Perić, X. Bombois, and L. Vanfretti, "Optimal multisine probing signal design for power system electromechanical mode estimation," in *Proc. 50th Hawaii Int. Conf. Syst. Sci.*, 2017, pp. 3156–3164.
[33] M. Forgione, X. Bombois, P. M. Van den Hof, and H. Hjalmarsson, "Experiment design for parameter estimation in nonlinear systems based on multilevel excitation," in *Proc. Eur. Control Conf. (ECC)*, Jun. 2014, pp. 25–30.
[34] *iTesla: Innovative Tools for Electrical System Security within Large Areas*. Accessed: Oct. 13, 2017. [Online]. Available: http://www.itesla-project.eu/

TETIANA BOGODOROVA (S'12) received the B.S. degree in computerized systems, automatics and control and the M.Sc. degree in automatic and control systems specialized in control theory from the National Technical University of Ukraine - Kyiv Polytechnic Institute. She is currently pursuing the Ph.D. degree with the Electrical Power Systems Division, School of Electric Engineering, KTH - Royal Institute of Technology, Stockholm.

Her experience includes the development of the operations support system for telecommunication industry as a System Engineer with the System Analytics Group, Research and Development, NetCracker Technology Corporation. Her current research interests lie on the intersection of system identification theory and power systems analysis, modeling, and validation.

LUIGI VANFRETTI (SM'15) was conferred the Swedish Title of Docent in 2012, where he was an Assistant Professor from 2010 to 2013. Since 2011, he has served as an Advisor of the Research and Development Division of Statnett SF, Oslo, Norway, where he is Special Advisor in Strategy and Public Affairs (SPA - Strategi og Samfunnskontakt). He is an Associate Professor (Tenured) and Docent with the Electric Power Systems Department, KTH Royal Institute of Technology, Stockholm, Sweden. His major research funded projects are IDE4L, Ideal Grid for All; FP7-Energy-2013-7-1-1 Call. PI for KTH funded by the European Commission; iTesla, Innovative Tools for Electric Power System Security within Large Areas; FP7-Energy-2011-1 Call. PI for KTH funded by the European Commission; STRONg2rid, Smart Transmission Grids Operation and Control; Funded by Nordic Energy Research and Svenska Kraftnät, Sustainable Energy Systems 2050 call. PI for KTH.

Prof. Vanfretti is mainly active in the Power and Energy Society, where he contributes to several working groups, task forces, and committees. He served, since 2009, in the IEEE Power and Energy Society PSDP Working Group on Power System Dynamic Measurements, where he is currently the Vice Chair. In addition, since 2009, he has served as the Vice Chair of the IEEE PES CAMS Task Force on Open Source Software.